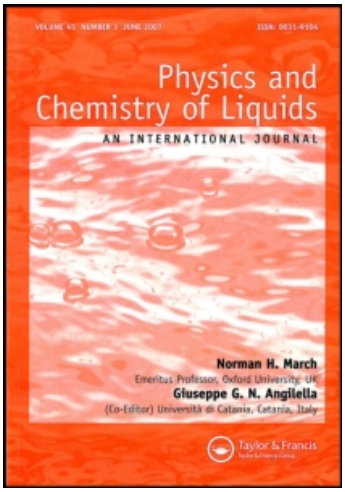

Physics and Chemistry of Liquids
Publication details, including instructions for authors and subscription information:
http://www.informaworld.com/smpp/title~content=t713646857

Neutron scattering and atomic dynamics in liquid nickel

M. W. Johnson[ab]; B. McCoy[a]; N. H. March[a]; D. I. Page[c]
[a] Department of Physics, The Blackett Laboratory, Imperial College, London [b] Neutron Beam Research Unit, Rutherford Laboratory, Chilton, Oxon [c] Material Physics Division, Oxon

To cite this Article Johnson, M. W. , McCoy, B. , March, N. H. and Page, D. I.(1977) 'Neutron scattering and atomic dynamics in liquid nickel', Physics and Chemistry of Liquids, 6: 4, 243 — 260
To link to this Article: DOI: 10.1080/00319107708084143
URL: http://dx.doi.org/10.1080/00319107708084143

Phys. Chem. Liq., 1977, Vol. 6, pp. 243–260

Printed in Holland

Neutron Scattering and Atomic Dynamics in Liquid Nickel

M. W. JOHNSON,† B. McCOY, N. H. MARCH

Department of Physics, The Blackett Laboratory, Imperial College, London

and D. I. PAGE

Materials Physics Division, Harwell, Didcot, Oxon.

(*Received August 24, 1976*)

The results of inelastic neutron scattering experiments on liquid nickel at a temperature of 1870°K are reported, one set of measurements being performed on natural nickel and another on an incoherently scattering mixture of nickel-58 and nickel-62 isotopes. From these data the dynamic structure factor $S(q, \omega)$ and the self function $S_s(q\ \omega)$ have been extracted over a limited range of q ($2.2 < q < 4.4$ Å^{-1}) and ω ($0 < \omega < 80$ meV).

To interpret $S_s(q, \omega)$ a model is used which attempts, as is usual, a precise description of the short-time behaviour of the atomic motions. The theory is characterized by two quantities for which first principles expressions are available. Because of uncertainties in (*a*) the interionic potential and (*b*) the static triplet correlation function, these two quantities are treated as parameters in the model. The main features of the incoherent scattering data are reflected by the model.

The coherent scattering data provides some preliminary evidence for the existence of collective modes in liquid nickel. Such modes, if they exist, would have to be due, at least in part, to the long-range force in the pair interaction, which has been estimated previously from the static structure factor $S(q)$.

Finally, approximations to $S(q, \omega)$ are calculated from the observed values of $S(q)$, using both measured data, and the model, for S_s and the usefulness and limitations of such relations are briefly assessed.

1 INTRODUCTION

The present series of neutron scattering experiments on liquid nickel was undertaken to measure both the dynamic structure factor $S(q, \omega)$ and the self-scattering function $S_s(q, \omega)$. This was done not only to give as complete a set of data as possible for basic liquid theory[1] but also

† Present address: Neutron Beam Research Unit, Rutherford Laboratory, Chilton, Oxon.

a) to determine the main features of the incoherent scattering which in the limit $q \to 0$ can be related to the spectral density function for the velocity autocorrelation function in the liquid, and

b) to look for evidence of collective modes of vibration in the liquid, i.e. excitations appearing in the coherent part of the scattering.

In section 2 the experimental procedures are described and the results given in graphical form† for $S(q, \omega)$ and $S_s(q, \omega)$ with an account of the corrections that have been applied to the raw data to obtain these scattering functions. Also in section 2, the possible existence of collective modes in the liquid, as seen in $S(q, \omega)$, is briefly discussed in relation to the form of the interionic potential derived from the static structure factor $S(q)$ by Johnson *et al.*[2]

Section 3 gives a two-parameter model calculation of the incoherent scattering, based on the generalized Langevin method of Mori.[3] From this the spectral density function is calculated (section 4) and compared with one estimated from the experimental data on both liquid and polycrystalline nickel. Section 5 outlines a route to generate $S(q, \omega)$ from $S_s(q, \omega)$ and $S(q)$ while finally comparison of some approximate relations is made with the experimental results.

2 EXPERIMENTAL PROCEDURES

The neutron scattering data are the results of two sets of experiments, one on a sample of natural nickel ($\sigma_{coh} = 13.33b$, $\sigma_{inc} = 4.04b$) and one on a mixture of nickel-58 and nickel-62 in which the isotopic abundances were such as to produce a wholly incoherent scatterer ($\sigma_{inc} = 15.75b$). The experiments were carried out on the twin chopper time-of-flight spectrometer on the Pluto reactor at Harwell[4] and a list of the relevant parameters is is given in Table I.

The most difficult problem was that of containing and heating small samples of liquid nickel without introducing too much extraneous material into the primary neutron beam. The final sample containers were tubes of Al_2O_3 or ZrO_2 produced by "plasma spraying" the material around a former‡:[5] each tube had an internal diameter of 6 mm and a wall thickness of 1 mm. The technique has the advantage that the mean density of the

† Tables of both S and S_s, as well as plots versus q at small intervals in ω are contained in Harwell report AERE/MPD/NBS/X which can be made available on request.

‡ We should like to thank Dr. K. T. Scott of the Material Development Division at Harwell for his sustained effort and interest.

TABLE I

Temperature	1870 (± 10) °K
Duration	21.7 hrs (natural Ni)
	30.3 hrs (incoherent Ni)
Mass	10.22 gm (natural Ni)
	6.24 gm (incoherent Ni)
Sample diameter	6.06 mm
Incident neutron	$\lambda = 2.05$ A°
	$E_0 = 19.23$ meV
	$\Delta E_0 = 3$ meV (FWHM)
Detectors	30 at 2° intervals from 38° to 96°
Beam dimensions	25 × 10 mm

sprayed material is lower (15%) than that of the normal solid, thus reducing the container scattering. Because of the small physical size of the sample the furnace heating element was also small, consisting of a tantalum cylinder of diameter 9.5 mm, length 150 mm and wall thickness 0.05 mm. No heat shields were used, in order to reduce the amount of the material in the neutron beam, and the running temperature of 1870°K was achieved with a power input of 0.5 kW (110 A at 5 V). Two thermocouples (26% and 5% Re in W) in contact with the base of the sample tube were used to control the power input.

The data corrections and reduction were carried out in the following stages:

i) The data were corrected for background, sample container and heater contribution, counter efficiency and Boltzmann factor (but not self-absorption, multiple scattering or resolution) using the data reduction programme CIRCA of Baston.[6] This program gives absolute values of the measured data by comparing it to the scattering from a standard vanadium sample. The output of this program is $\tilde{S}(q, \omega)_{\theta, \tau}$ where the subscripts indicate that the data are at equal intervals in scattering angle θ and time-of flight τ. (The usual non-linear τ^4 transformation was involved here)

ii) A series of cubic splines was fitted to the constant θ data using the Harwell subroutine VC ϕ 3A of Hopper[7] and from these values $\tilde{S}(q, \omega)_{\theta, \omega}$ were obtained by interpolation.

iii) The resolution function of the instrument was calculated following Royston[8] and deconvoluted values of $\tilde{S}(q, \omega)_{\theta, \omega}$ were obtained using the "moments method" of Johnson.[9] To give some idea of the size of the resolution correction, the ratio of the width at half maximum height of the observed spectra to the resolution function varied from 1.5 ($\theta = 38°$) to 6 ($\theta = 96°$).

iv) Values of $\tilde{S}(q, \omega)_{q, \omega}$ were obtained by again using subroutine VC ϕ 3 A to interpolate along constant ω contours.

v) These values were used as input to the multiple scattering correction program DISCUS.[10] Since $S(q, \omega)$ could only be measured between scattering angles of 38° and 96°, it was necessary to extend the $\tilde{S}(q, \omega)$ surface to higher and lower scattering angles in order to perform a realistic calculation. The regions of the $q - \omega$ plane used in the DISCUS calculation were

$$-70 < \omega < +70 \text{ meV}, 0.2 < q < 6.0 \text{ Å}^{-1} \text{ (incoherent Ni)}$$

and

$$-70 < \omega < +70 \text{ meV}, 2.0 < q < 6.0 \text{ Å}^{-1} \text{ (natural Ni)}$$

The surface was extrapolated beyond the measured values by assuming $S(q, \omega)_{q,\omega}$ to be Lorentzian (justified to some extent for S_s from hydrodynamics) in shape for angles less than the minimum experimental angle, and Gaussian shaped for angles greater than the maximum experimental angle.

The DISCUS program was used in a mode that corrected for multiple scattering and absorption in the sample. The output from the program was a series of numbers $R_{\theta,\omega}$; the ratio of the "ideal" flux to the observed flux (where the ideal flux is that which would be observed if neutrons were forbidden to undergo multiple scattering and the absorption cross-section was zero). The multiple scattering correction varied widely over the (q, ω) plane. Near the elastic peak, the correction was $<10\%$. At the highest energy transfer, the correction reached 40%.

vi) The values of $R_{\theta,\omega}$ were interpolated on to a $R_{q,\omega}$ grid and used to correct the output of stage (iv). The corrected values of $\tilde{S}_s(q, \omega)$ and $\tilde{S}(q, \omega)$ are shown in the form of three-dimensional plots in Figures 2.1 and 2.2. In the case of the natural nickel sample, the results contained a small fraction of incoherent scattering—this has been subtracted at the final stage (vi) to give completely coherent values.

The data are presented with no indicated errors because the involved data correction procedure makes their calculation particularly difficult. The error due to counting statistics is $\sim 5\%$; this was confirmed by comparing values of $S(q, \pm\omega)$ and $S_s(q, \pm\omega)$ (i.e., a first moment check) for which the standard deviation was 5% and 4% respectively. Errors in the zeroth moment of 6% for $S(q, \omega)$ and 4% for $S_s(q, \omega)$ reflect the fact that multiple scattering effects are more important in the former. Attempts were made to calculate the second moments, but it was realized that an insufficient region of (q, ω) space was covered to allow complete integration of the data. Integration out to $\omega = \pm 80$ meV at the highest observed q-values (4.4 Å^{-1}) gave the correct theoretical value but the integrated area was still not closed. This leads

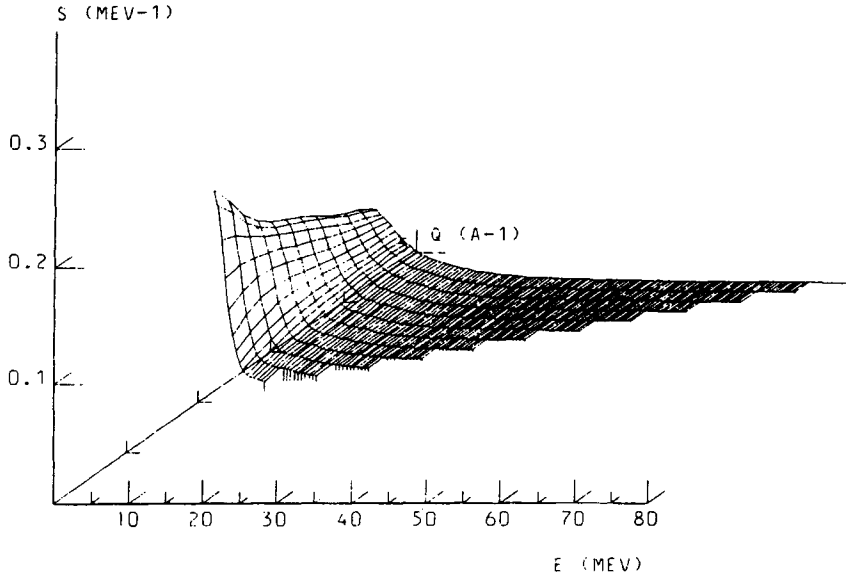

FIGURE 2.1 Three-dimensional representation of $S_s(q, \omega)$.

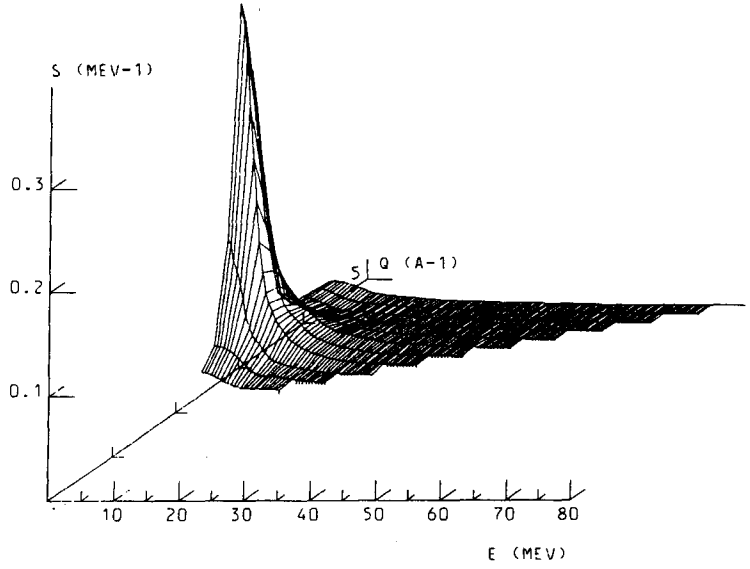

FIGURE 2.2 Three-dimensional representation of $S(q\ \omega)$.

us to believe that the experimental values are increasingly in error at high values of ω, with $\sim 20\%$ error at $\omega = \pm 80$ meV. This is due almost certainly to the inherent inaccuracies in the multiple scattering correction.

In Figure 2.3 which shows $S(q, \omega)$ at constant detected angle before correction for resolution or multiple scattering effects, small maxima can be seen at $q < 3$ Å^{-1} and $\omega \sim 10$ meV which persist over several detectors (the third and the fifth especially). These are somewhat suggestive of collective excitations in the liquid, though less decisive evidence than that presented for liquid rubidium by Copley and Rowe.[11] There are three cautionary remarks therefore in connection with this experiment on liquid Ni:

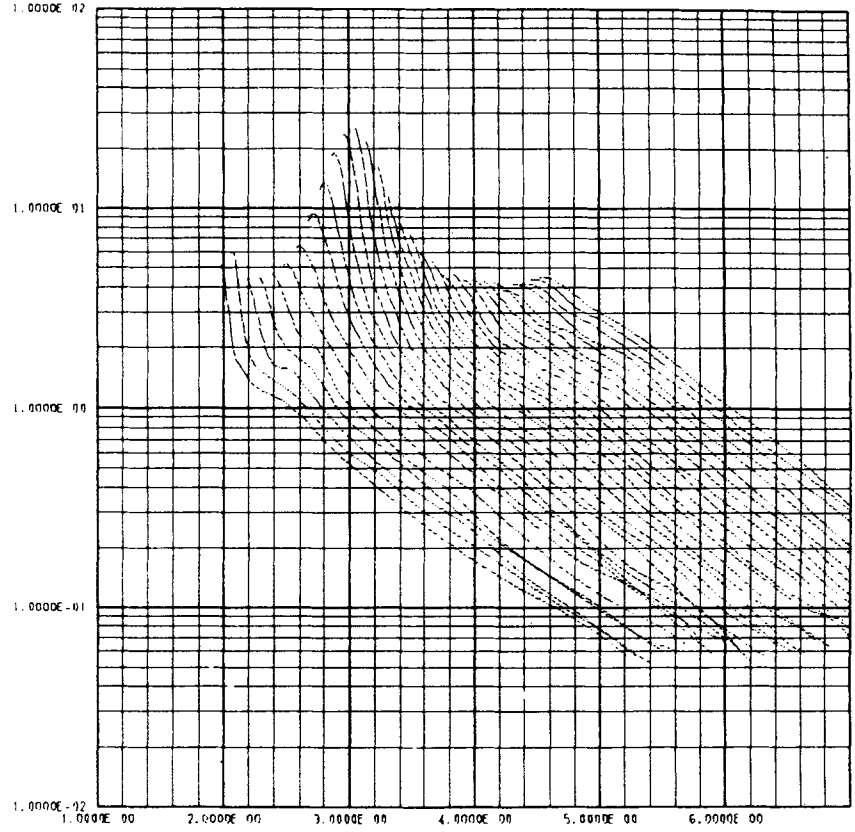

FIGURE 2.3 $S(q, \omega)$ as a function of energy transfer $\hbar\omega$ at constant angle. (For $S(q, \omega)$ in absolute units, see Figure 2.2. The present Figure is shown primarily in connection with the discussion on the possible existence of collective excitations).

Each curve represents the data from a single detector and is not corrected for resolution or multiple scattering.

a) The bumps seem to be significant primarily for the third and fifth detectors only.

b) There are some bumps of comparable size in some of the other detectors, at similar values of the intensity: i.e., the statistics are comparable. Thus there must be some question about placing too much emphasis on the bumps found in the lower angle detectors.

c) The curves are at constant angle, not constant q. It is possible for constant angle curves, under some circumstances, to display "spurious" peaks, especially if q is a little smaller than q_0, where the static structure factor $S(q)$ has its main peak. These peaks can result from the detailed topology of the $S(q, \omega)$ surface.

In view of all this, a study specifically in the range $0 < q < 3$ Å^{-1} should be undertaken with a view to obtaining decisive evidence on whether or not collective excitations exist in liquid nickel. Conversely, in the experimental data for liquid argon obtained by Skold *et al.*[1] there is no evidence for collective modes for larger q's than those for which sound waves propagate. Although the nickel interionic potential has an exceptionally hard core due to the large d-shells it also, in marked contrast to the argon potential, has a long-range attractive part as shown by Johnson *et al.*[2] Any collective effects would have to be due, at least in part, to this longer range force in liquid nickel.†

3 MEMORY FUNCTION DESCRIPTION OF INTERMEDIATE SCATTERING FUNCTION

Despite the fact that liquid nickel should be treated as a two-component system of electrons and ions, we will make the simpler assumption that it can be treated as a classical liquid with ions interacting through an effective pair potential. The long-range features already referred to will clearly be mediated by the itinerant electrons.

It will be useful to work with the time Fourier transforms $I(q, t)$ and $I_s(q, t)$ of $S(q, \omega)$ and $S_s(q, \omega)$ respectively. Furthermore, following van Hove[12] the total intermediate scattering function $I(q, t)$ will be written as the sum of a distinct part $I_d(q, t)$ and $I_s(q, t)$. Then Mori[3] has shown that

$$\frac{\partial}{\partial t} I_s^{(n)}(q, t) + \int_0^t \mathrm{d}\tau I_s^{(n+1)}(q, \tau) I_s^{(n)}(q, t - \tau) = 0; n = 0, 1, 2, \ldots, \quad (3.1)$$

† Further analysis of the small maxima in Figure 2.3 is presented in Harwell Report AERE/MPD/NBS/X.

where $I_s^{(0)}(q, t) = I_s(q, t)$. $I_s^{(n)}(q, t)$ for $n \geq 1$ can be regarded as the nth order memory function. To solve Eq. (3.1) for a given n, the initial values $I_s^{(n)}(q, t = 0)$ are needed; for small n one finds

$$I_s(q, 0) = 1; I_s^{(1)}(q, 0) = \frac{q^2}{M\beta}, \beta = (k_B T)^{-1}$$

$$I_s^{(2)}(q, 0) = \frac{\beta D(0)}{M} + \frac{2q^2}{M\beta} \tag{3.2}$$

$$I_s^{(3)}(q, 0) = \frac{6\left(\frac{q^2}{M\beta}\right)^2 + \frac{9\beta D(0)}{M}\left(\frac{q^2}{M\beta}\right) + \mathscr{T} - \left(\frac{\beta D(0)}{M}\right)^2}{\frac{\beta D(0)}{M} + \frac{2q^2}{M\beta}}$$

These results are equivalent to the moment theorems, $I_s^{(2)}$ being a linear combination of second and fourth moments for example. In Eq. (3.2), $D(0)$ and $\mathscr{T}$ are equilibrium constants, the explicit forms being given in the Appendix. $D(0)$ depends of the radial distribution function $g(r)$ and the pair potential $\phi(r)$ and will be calculable once an accurate $\phi(r)$ exists. But $\mathscr{T}$ depends on equilibrium triplet correlations and is only calculable in terms of some approximate result such as the Kirkwood superposition. It is useful in what follows therefore to view $D(0)$ and $\mathscr{T}$ as two parameters characterizing our model.

In a similar manner one obtains

$$I(q, 0) = S(q); I^{(1)}(q, 0) = \frac{q^2}{M\beta S(q)}$$

$$I^{(2)}(q, 0) = \frac{\beta D(0)}{M} - \frac{\beta D(q)}{M} + \frac{q^2}{M\beta}\left[3 - \frac{1}{S(q)}\right] \tag{3.3}$$

where $D(q)$ is recorded in the Appendix in terms of $g(r)$ and $\phi(r)$.

4 COMPARISON OF INCOHERENT SCATTERING MODEL WITH EXPERIMENT

4.1 Model of the incoherent scattering

Existing models of S_s are discussed by Copley and Lovesey.[13] Here we shall use the hierarchy given in Eq. (3.1) to obtain a somewhat different model for $S_s(q, \omega)$ which we shall also use below to discuss $S(q, \omega)$. Defining $I_s^{(n+)}(q, \omega)$ to be the Fourier integral between 0 and infinity of $I_s^{(n)}(q, t)$ and $I_s^{(n-)}$ as the one-sided Fourier transform from $-\infty$ to 0, the incoherent

scattering $S_s(q, \omega)$ is simply the sum of $I_s^{(0+)}(q, \omega)$ and $I_s^{(0-)})(q, \omega)$. The relation of $I_s^{(n\pm)}$ to $I_s^{(n)}$ is readily shown to be

$$I_s^{(n\pm)}(q, \omega) = \frac{I_s^{(n)}(q, t = 0)}{\pm i\omega + I_s^{(n+1\pm)}(q, \omega)}. \tag{4.1.1}$$

Applying this to $n = 1$, and defining X and Y as the cosine and sine transforms of $I_s^{(2)}(q, t)$ respectively, the use of the initial condition for $I_s^{(1)}$ (see Eq. (3.2)) gives the result

$$S_s(q, \omega) = \frac{\dfrac{q^2}{\pi M\beta}\dfrac{X}{X^2 + (\omega - Y)^2}}{\left[\dfrac{q^2}{M\beta}\dfrac{X}{X^2 + (\omega - Y)^2}\right]^2 + \left[\omega - \dfrac{q^2}{M\beta}\dfrac{(\omega - Y)}{X^2 + (\omega - Y)^2}\right]^2} \tag{4.1.2}$$

To evaluate this equation we must now introduce a model for $I_s^{(2)}(q, t)$. The highest order sum rule which can be usefully imposed on $I_s^{(2)}$ with presently available information is equivalent to

$$\frac{\partial^2}{\partial t^2} I_s^{(2)}(q, t)\bigg|_{t=0} = -I_s^{(3)}(q, t = 0) I_s^{(2)}(q, t = 0), \tag{4.1.3}$$

the lower order sum rules having already been accounted for. The simplest assumption satisfying Eq. (4.1.3) is to write

$$I_s^{(2)}(q, t) \doteq I_s^{(2)}(q, t = 0)\exp\left(\frac{-t^2}{2} I_s^{(3)}(q, t = 0)\right). \tag{4.1.4}$$

One then readily obtains

$$X(q, \omega) = A(q)\left\{\frac{\pi}{2B(q)}\right\}^{1/2} \exp\left(\frac{-\omega^2}{2B(q)}\right)$$

and $\tag{4.1.5}$

$$Y(q, \omega) = \frac{A(q)}{B(q)} \exp\left(\frac{-\omega^2}{2B(q)}\right)\Phi\left(\frac{1}{2}, \frac{3}{2}; \frac{\omega^2}{2B(q)}\right)$$

where Φ is the degenerate hypergeometric function[14] while A and B are simply written for the initial values of $I_s^{(2)}$ and $I_s^{(3)}$ respectively. For finite q and sufficiently large ω, Eq. (4.1.5) shows an exponential decay of $X(q, \omega)$ with ω^2.

Using Eq. (4.1.5) in Eq. (4.1.2) S_s has been evaluated and compared with experiment. In this evaluation the theoretical S_s has been adjusted to the

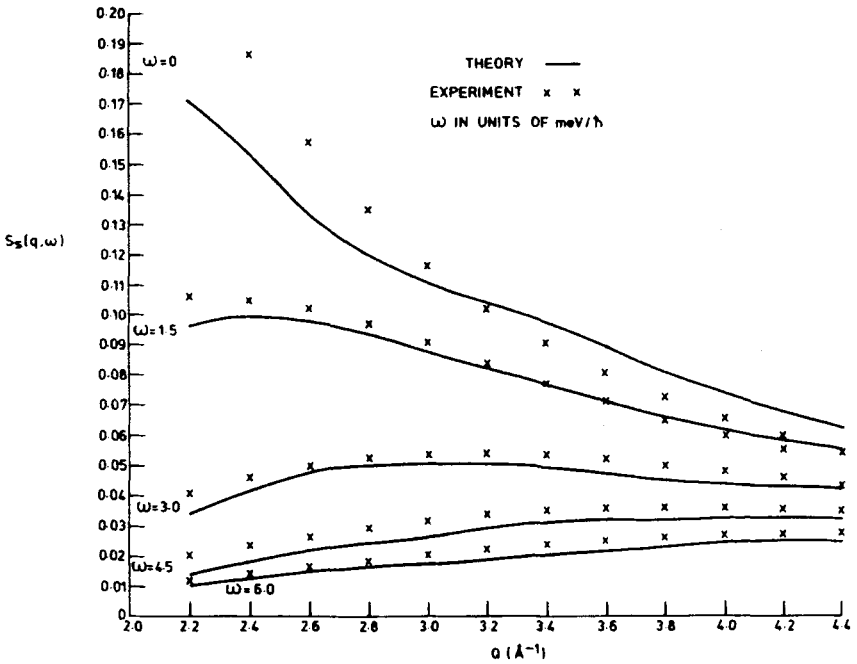

FIGURE 4.1 Plots of $S_s(q, \omega)$ at constant values of ω. Units of S_s are $\hbar(\text{meV})^{-1}$. Crosses: Neutron experiment. Curves: calculated from Eqs. (4.1.2) and (4.1.5), with parameters D(0) and $\mathscr{T}$ quoted in text.

experimental data, yielding values of $D(0)$ and $\mathscr{T}$ given by

$$\frac{\beta D(0)}{M} = 0.22 \times 10^{28}\ \text{sec}^{-2}; \mathscr{T} - \left\{\frac{\beta D(0)}{M}\right\}^2 = 0.40 \times 10^{55}\ \text{sec}^{-4}.$$

The main features of the experiment are reflected in the model as shown in Figure 4.1. It should be noted that at large energy transfers, the experimental data decays exponentially with ω, confirming at least qualitatively the form of Eq. (4.15) in this limit. However, in detail, as we shall see below, the model S_s falls off too rapidly at very large energy transfers.

4.2 Spectral density function

The spectral density function $g(\omega)$, defined as the Fourier transform of the velocity autocorrelation function can be estimated from $S_s(q, \omega)$ in the long wavelength limit by[15]

$$g(\omega) = 2M\beta \lim_{q \to 0} \frac{\omega^2}{q^2} S_s(q, \omega). \tag{4.2.1}$$

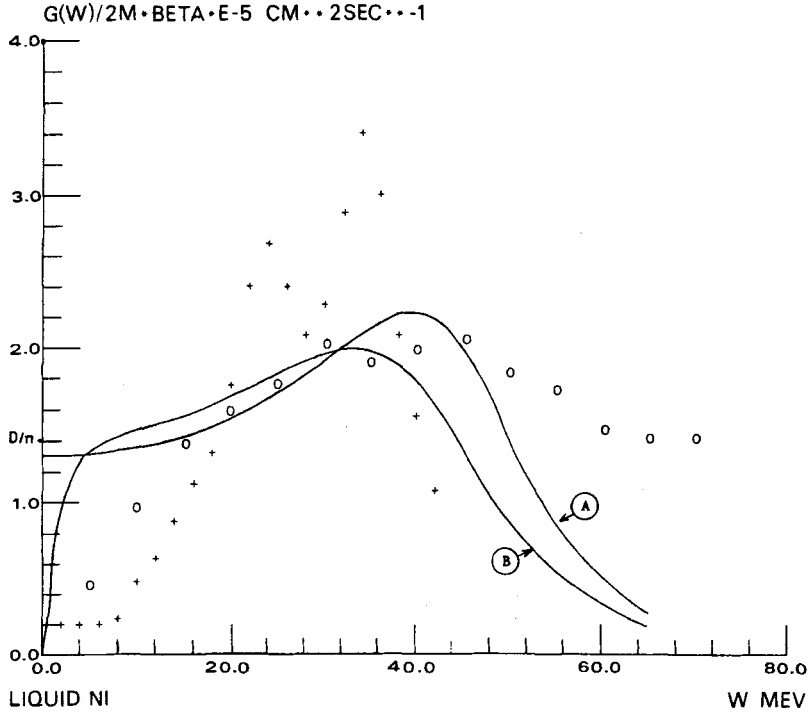

FIGURE 4.2 Spectral density function $g(\omega)$. Curve A: From model $S_s(q, \omega)$ in $q \to 0$ limit. Curve B: From model $S_s(q, \omega)$ at $q = 2.2$ Å^{-1}. Circles: From liquid measurements at $q = 2.2$ Å^{-1}. Crosses: For polycrystalline nickel.

This expression has been calculated using Eq. (4.1.5) for X and Y, with the parameter values already given. The result is shown in Figure 4.2 as the solid line A. It is satisfactory that the intercept at $\omega = 0$ is close to D/π, where D is the self-diffusion constant, though not surprising since $D(0)$ and $\mathcal{T}$ were obtained by fitting to the measurements while D was obtained from the analysis of the measured widths of the incoherent quasi-elastic peaks as a function of momentum transfer. To our knowledge, direct measurements of D in liquid nickel do not exist. It would be useful to have them, to compare with the above value; the agreement should not be expected to be fully quantitative however, for we have extracted D from $S_s(q, \omega)$ at quite substantial values of q, rather than from $q \to 0$ data.

Related to this, an estimate of $g(\omega)$ can be obtained from the experimental data using Eq. (4.2.1) by ignoring the limit $q \to 0$. Ignoring this limit will introduce a multiphonon contribution into the estimate which will be large in our case at high excitations due to the temperature dependence of the Boltzmann factor. Thus we expect our estimate of $g(\omega)$ to be increasingly

in error at increasing energy transfers. We also apply a lower energy cutoff of $\omega = 8$ meV as we can draw no conclusions as to the diffusive modes.

To investigate the effect of calculating $g(\omega)$ when $q \neq 0$, curve B in Figure 4.2 has been calculated from the model (4.1.2) for $S_s(q, \omega)$ at $q = 2.2$ Å^{-1}. The agreement with curve A is good between $\omega = 10$ and 40 meV.

For comparison, the frequency distribution of the polycrystalline solid[16] is also shown (crosses). The liquid measurements (circles) are in fair agreement with theory between 15 and 50 meV but at large ω diverge from both the model and the values for the solid as expected. The discrepancy between curve B and the circles is a consequence of the Gaussian ω dependence of X in Eq. (4.1.5).

In concluding this part of the discussion, we want to stress that the assumption (4.1.4) has a limited range of validity in t. Thus, we know that, from the existence of long time tails in the velocity autocorrelation function, $g(\omega) = D/\pi + 0(\omega^{1/2})$ at sufficiently small ω, as discussed for example by March and Tosi.[17] It must not be expected that the Gaussian form (Eq. 4.1.4) is useful for such detailed purposes. However, we have been mainly concerned with that region of the (q, ω) plane accessible to neutron scattering and here it seems that Eq. (4.1.4) is useful in representing the frequency behaviour at least up to about 40 meV.

5 RELATION BETWEEN S_s AND $S(q, \omega)$

5.1 Earlier work

It is entirely possible to develop a model for $S(q, \omega)$ in a manner analogous to that given in section 4 for $S_s(q, \omega)$. However, instead we shall consider whether the present experimental data supports a number of microscopic theories (e.g., Vineyard,[18] Kerr,[19] Hubbard and Beeby,[20] Gyorffy and March[21] and numerous later workers). The viewpoint of these theories is that $S(q, \omega)$ can be usefully expressed in terms of the incoherent scattering function $S_s(q, \omega)$ and static correlation functions. We shall consider below two versions of this class of theory. The most elementary form, which turns out to be closely related to Vineyard's theory, is a *linear* relation between $S(q, \omega)$ and S_s.

5.2 Linear relation between S and S_s

The distinct intermediate scattering function $I_d(q, t)$ may be shown to have the form

$$I_d(q, t) = \langle a(q, 0), e^{i\mathbf{q}\cdot\mathbf{x}_s(t)} \rangle \qquad (5.2.1)$$

where $a(q, t)$ is defined by

$$a(q, t) = (N - 1)[e^{i\mathbf{q}\cdot\mathbf{x}_j(t)} - 1]. \tag{5.2.2}$$

We now use the generalized forces $f_n(q, t = 0)$ at $t = 0$, which as Mori[3] has shown, form a complete, orthogonal set of functions. Then we can write Eq. (5.2.1) as

$$I_s(q, t) = \sum_{n=0}^{\infty} \frac{\langle a(q, 0), f_n(q, 0)\rangle \langle f_n(q, 0), f_0(q, -t)\rangle}{\langle f_n(q, 0), f_n(q, 0)\rangle} \tag{5.2.3}$$

where we have inserted the completeness relation

$$1 = \sum_{n=0}^{\infty} \frac{|f_n(q, 0)\rangle \langle f_n(q, 0)|}{\langle f_n(q, 0), f_n(q, 0)\rangle}. \tag{5.2.4}$$

The $n = 0$ term in Eq. (5.2.3) is simply $[S(q) - 1]I_s(q, t)$. If we assume that there is a range of the (q, t) plane over which the leading term dominates then we find

$$I(q, t) \simeq S(q)I_s(q, t) \tag{5.2.5}$$

which yields Vineyard's well known approximation

$$S(q, \omega) \simeq S(q)S_s(q, \omega). \tag{5.2.6}$$

This all suggests (since n odd terms vanish identically) that one might correct the Vineyard result (5.2.5) with the $n = 2$ term in Eq. (5.2.3). Fourier transforming this term, and adding to Eq. (5.2.5) yields in the next order

$$S(q, \omega) \simeq \left\{ S(q) + \frac{\{S(q) - 1\}}{\left[\frac{\beta D(0)}{M} + \frac{2q^2}{M\beta}\right]} \left[\frac{q^2}{M\beta} - \omega^2\right] \right\} S_s(q, \omega) \tag{5.2.7}$$

Two points may be noted from Eq. (5.2.7). First, when $S(q)$ intersects its asymptotic value unity, S becomes equal to S_s, as with Vineyard. However, near the first peak of $S(q)$, Eq. (5.2.7) could lead to a negative value of $S(q, \omega)$ for sufficiently large ω and is clearly not valid unless $\omega^2 < q^2/M\beta$.

The Vineyard theory is shown in Figure 5.1 (crosses) by using $S(q)$ and S_s from experiment. The agreement with the measured coherent scattering is quite good near the principal peak for $\omega = 0$. The corrections given in Eq. (5.2.7) are shown by the circles and are small.

Returning to Eq. (5.2.3) the factor $\langle f_n(q, 0), f_0(q, -t)\rangle$ can be expressed as an even polynomial of the time derivative operating on $I_s(q, t)$ for even n. Hence on Fourier transforming a linear relation between S and S_s is found, in the form of a power series in ω, the coefficients of which depend on static correlation functions. However, ω^2 appears in *all* the terms in the sum.

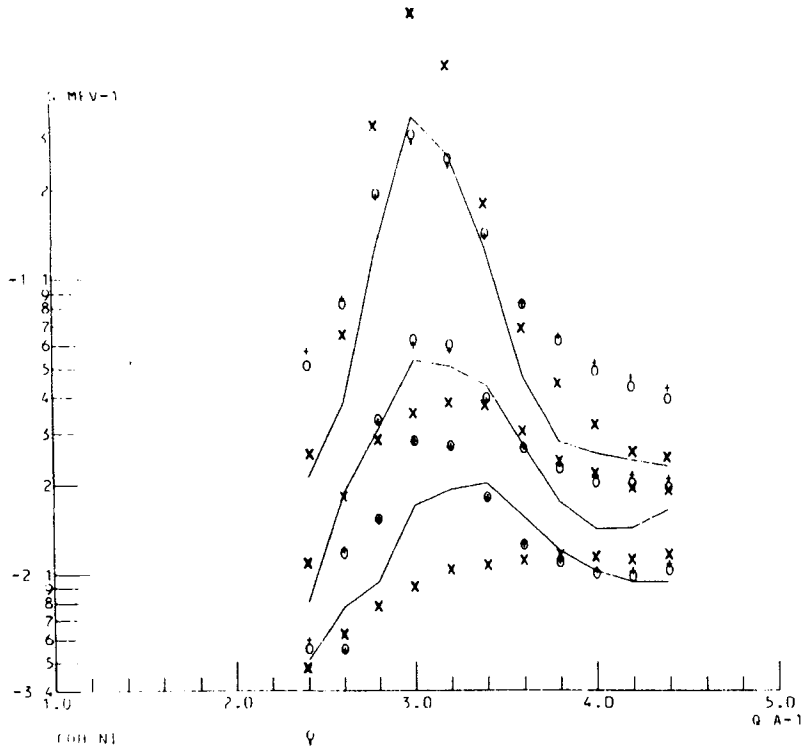

FIGURE 5.1 Coherent scattering function $S(q, \omega)$ at constant values of ω. Solid curves: experimental results at $\omega = 0$ (upper curve), 5 and 10 meV. Crosses (+): Vineyard theory. Circles: Linear theory (5.2.7) correcting Vineyard. Diagonal crosses (×): Theory of Eq. (5.4.5).

Unfortunately, the denominators $\langle f_n(q, 0), f_n(q, 0)\rangle$ involve higher order equilibrium correlation functions for increasing n. For this reason, it seems *unlikely* that a simple and useful linear relation exists between S and S_s except over a quite limited region of the (q, ω) plane.

5.3 Non-linear forms for S in terms of S_s

We now consider non-linear relationships between $S(q, \omega)$ and $S_s(q, \omega)$ plus the static correlations.

The hierarchy of equations of the form (3.2) is amenable to solution by Laplace transformation. Thus we introduce

$$I^{(n)}(q, p) \equiv \int_0^\infty \mathrm{d}t e^{-pt} I^{(n)}(q, t) \tag{5.3.1}$$

If we assume the existence of a linear, time independent relation between $I(t,7)$ and $I_s(q,t)$ then we must have

$$\begin{aligned} I(q,t) &\simeq \frac{I(q,t=0)}{I_s(q,t=0)} I_s(q,t) \\ &= S(q) I_s(q,t) \end{aligned} \tag{5.3.2}$$

which is again Vineyard's approximation.

To attempt a refinement of this, let us assume, by analogy with the above argument, that a linear, time independent relation exists between the two (first-order) memory functions $I^{(1)}$ and $I_s^{(1)}$. Then we must have

$$I^{(1)}(q,t) \simeq \frac{I^{(1)}(q,t=0)}{I_s^{(1)}(q,t=0)} I_s^{(1)}(q,t) \tag{5.3.3}$$

which implies that

$$I^{(1)}(q,p) \simeq \frac{I_s^{(1)}(q,p)}{S(q)}. \tag{5.3.4}$$

This leads to[19]

$$I(q,p) \approx \frac{S^2(q) I_s(q,p)}{1 + pI^s(q,p)[S(q) - 1]}. \tag{5.3.5}$$

Clearly, for a full test of Eq. (5.3.5) the present measurements will have to be extended to cover a substantially greater area of the $(q\omega)$ plane. However, in the following section, we show how the use of the model for S_s can bring this relation into contact with experiment.

5.4 Test of non-linear relation

The result (5.3.5) reads

$$I^{\pm}(q,\omega) \simeq \frac{S^2(q) I_s^{\pm}(q,\omega)}{1 \pm i\omega I_s^{\pm}(q,\omega)[S(q) - 1]} \tag{5.4.1}$$

We now write

$$I_s^{\pm}(q,\omega) = U(q,\omega) \mp iV(q,\omega) \tag{5.4.2}$$

and using the model of incoherent scattering we find that

$$U(q,\omega) = \frac{\dfrac{q^2}{M\beta} \dfrac{X}{X^2 + (\omega - Y)^2}}{\left[\dfrac{q^2}{M\beta} \dfrac{X}{X^2 + (\omega - Y)^2}\right]^2 + \left[\omega - \dfrac{q^2}{M\beta} \dfrac{(\omega - Y)}{X^2 + (\omega - Y)^2}\right]^2} \tag{5.4.3}$$

and

$$V(q,\omega) = \frac{\omega - \dfrac{q^2}{M\beta}\dfrac{(\omega - Y)}{X^2 + (\omega - Y)^2}}{\left[\dfrac{q^2}{M\beta}\dfrac{X}{X^2 + (\omega - Y)^2}\right]^2 + \left[\omega - \dfrac{q^2}{M\beta}\dfrac{(\omega - Y)}{X^2 + (\omega - Y)^2}\right]^2} \tag{5.4.4}$$

Then we find

$$S(q,\omega) = \frac{1}{\pi}\frac{S^2(q)U}{[1 + \omega(S(q) - 1)V]^2 + [\omega(S(q) - 1)U]^2} \tag{5.4.5}$$

This expression has been evaluated and compared with experiment. Before presenting the main results for the region of the (q, ω) plane covered by the neutron scattering experiment, we emphasize that the theory is not designed to work in the hydrodynamic regime, where, of course, the form of $S(q, \omega)$ is well known. In particular, at small q and ω, Eq. (5.3.5) becomes inapplicable.

The results of Eq. (5.4.5) are plotted in Figure 5.1, for $\omega = 0$, 5 and 10 meV. It can be seen that Eq. (5.4.5) substantially overestimates the elastic scattering around the peak in $S(q)$. Here Vineyard's result is in better agreement with experiment but the non-linear theory is an improvement at q values greater than 3 A^{-1}, for $\omega = 0$.

For non-zero energy transfers ($\hbar\omega = 5$ and 10 meV) Vineyard's theory now overestimates the main peak whereas the non-linear theory gives too little structure.

6 SUMMARY AND CONCLUSIONS

From neutron scattering experiments, the dynamic structure factor $S(q, \omega)$ and the self scattering function $S_s(q, \omega)$ have been measured for liquid nickel over a range in the (q, ω) plane from $2.2 < q < 4.4$ A^{-1}; $0 < \hbar\omega < 80$ meV.

These functions are interpreted using Mori's generalized Langevin equation approach. The incoherent scattering is reduced to a two-parameter model, where in principle the parameters ($D(0)$ and $\mathcal{T}$) are calculable from $g(r)$, $\phi(r)$ and the three-body correlation function g_3. From this model the frequency spectrum $g(\omega)$ is calculated. With the two parameters chosen to fit $S_s(q, \omega)$, the diffusion constant D(measured as 4.6×10^{-5} cm^2/sec) is quantitatively given by $\pi g(0)$. Secondly, the liquid frequency spectrum estimated from the measured S_s at $q = 2.2$ A^{-1} is in quantitative accord with the same model between $\hbar\omega = 15$ meV and 45 meV.

The modelling of the dynamical structure factor $S(q, \omega)$ is less complete, but some understanding of the experiments is afforded by relating $S(q, \omega)$

to $S_s(q, \omega)$ and the static structure factor. Future theory of $S(q, \omega)$ for liquid nickel will have to incorporate explicitly the long range part of $\phi(r)$, especially if later work confirms the existence of collective excitations at large values of q.

Acknowledgment

We are grateful to Dr Peter Grout for his considerable help and advice with the numerical aspects of this work. Dr J. Copley made some useful comments on an earlier draft of the paper.

Appendix The equilibrium structure constants

The equilibrium constant $D(0)$ entering the present theory of the self function $S_s(q\omega)$ is, essentially the average value of the square of the force. Specifically

$$D(0) = \langle F_1 F_1 \rangle_{eq} \tag{A.1}$$

where F_1 is the total force acting on particle 1.

The second equilibrium constant $\mathscr{T}$ entering $S_s(q\omega)$ is a more complicated functional of the force, namely

$$\mathscr{T} = \frac{1}{M^2} \sum_{k=1}^{N} \langle (\nabla_k F_1^x) \cdot (\nabla_k F_1^x) \rangle_{eq}. \tag{A.2}$$

We shall not go into detail about $\mathscr{T}$, as it involves the static triplet correlation function in an essential way. At present, therefore, we cannot calculate it without making some approximation such as the Kirkwood superposition and we have preferred in the body of the text to view $\mathscr{T}$ (and also $D(0)$) as a parameter involved in modelling $S_s(q, \omega)$.

In contrast $D(0)$ is, in principle, calculable from first principles. Thus, in terms of the pair potential $\phi(r)$ we define

$$J(r) = \frac{1}{r}\frac{d\phi}{dr}; K(r) = \frac{1}{r}\frac{dJ}{dr} \tag{A.3}$$

when we find

$$D(0) = \frac{4\pi M}{\beta} \int_0^\infty dr g(r) \left[r^2 J(r) + \frac{r^4}{3} K(r) \right] \tag{A.4}$$

Eqs. (A.3) and (A.4) reveal that while $\beta D(0)/M$ can be calculated by quadrature from a knowledge of $g(r)$ and $\phi(r)$, the second derivative of ϕ is involved. With the accuracy of the presently known potential of Johnson *et al.*[2] we do not feel it is justifiable to rely on evaluation of $D(0)$ from Eq. (A.4)

and, as with $\mathscr{T}$, we have regarded it as the second parameter characterising our model of $S_s(q, \omega)$.

The non-zero wave number generalization $D(q)$ (see Eq. 3.3) of $D(0)$ may be worth recording for future work, namely

$$D(q) = \frac{4\pi M}{\beta}\left\{\int_0^\infty \mathrm{d}r\, r^2 g(r)\left[\frac{J(r)\sin qr}{qr} - \frac{K(r)}{q^2}\left(\frac{2\sin qr}{qr} - 2\cos qr - \sin qr\right)\right]\right\} \tag{A5}$$

which reduces to Eq. (A4) in the limit $q \to 0$.

References

1. Compare K. Skold, J. M. Rowe, G. Ostrowski, and P. D. Randolph, *Phys. Rev.*, **A6**, 1107 (1972).
2. M. W. Johnson, N. H. March, B. McCoy, S. K. Mitra, D. I. Page, and R. C. Perrin, *Phil. Mag.*, **33**, 203 (1976).
3. H. Mori, *Prog. Theor. Phys.*, **34**, 399 (1965).
4. Science Research Council, *Neutron beam facilities available for University users at UKAEA Establishments* (1973).
5. R. F. Smart and J. A. Catherall, *Plasma spraying*, Mills and Boon Ltd. (1972).
6. A. M. Baston, *AERE Report*, M2570 (1972).
7. M. J. Hopper, *AERE Report*, R6912 (1971).
8. R. J. Royston, *Nuclear instruments and methods*, **30**, 184 (1964).
9. M. W. Johnson, Rutherford report (in press) (1976).
10. M. W. Johnson, *AERE Report*, R7682 (1974).
11. J. R. D. Copley and J. M. Rowe, *Phys. Rev.*, **A9**, 1656 (1974).
12. L. van Hove, *Phys. Rev.*, **95**, 249 (1954).
13. J. R. D. Copley and S. W. Lovesey, *Rep. Prog. Phys.*, **38**, 461 (1975).
14. Gradshteyn and Ryznik, *Tables of Integrals, Series and Products*, Academic Press, (1965).
15. P. A. Egelstaff, *An Introduction to the Liquid State*, Interscience, New York, 1967.
16. R. J. Birgeneau, J. Cordes, G. Dolling and A. D. W. Woods, *Phys. Rev.* **136**, A1359 (1964).
17. N. H. March and M. P. Tosi, *Atomic Dynamics in Liquids*, MacMillan, London, (1976).
18. G. H. Vineyard, *Phys. Rev.*, **110**, 999 (1958).
19. W. Kerr, *Phys. Rev.*, **174**, 316 (1968).
20. J. Hubbard and J. L. Beeby, *J. Phys.*, **C2**, 556 (1969).
21. B. L. Gyorffy and N. H. March, *Physics and Chemistry of Liquids*, **2**, 197 (1971).